Front. Environ. Sci. Eng. 2023, 17(1): 4
https://doi.org/10.1007/s11783-023-1604-5

RESEARCH ARTICLE

Time-dependent metabolomics uncover dynamic metabolic adaptions in MCF-7 cells exposed to bisphenol A

Haoduo Zhao[1,2], Min Liu[1,2], Junjie Yang[1,2], Yuyang Chen[3], Mingliang Fang (✉)[1,4]

1 School of Civil and Environmental Engineering, Nanyang Technological University, Singapore 639798, Singapore
2 Nanyang Environment & Water Research Institute, Nanyang Technological University, Singapore 637141, Singapore
3 School of Environmental Science and Engineering, Southern University of Science and Technology, Shenzhen 518055, China
4 Department of Environmental Science and Engineering, Fudan University, Shanghai 200433, China

HIGHLIGHTS

- Metabolomic temporal profiling of cells exposed to xenobiotics.
- Global metabolome dysregulation patterns with time-resolved landscapes.
- Synchronized regulation behavior and specific dysregulation sensitivity.
- Temporal metabolic adaptions indicated cellular emphasis transition.

GRAPHIC ABSTRACT

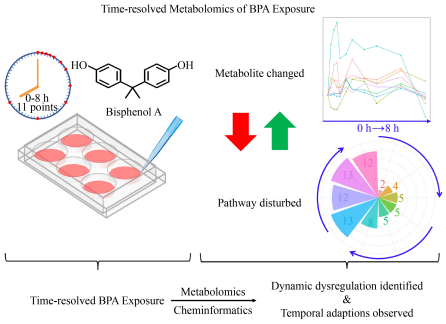

ARTICLE INFO

Article history:
Received 9 April 2022
Revised 24 May 2022
Accepted 13 June 2022
Available online 1 August 2022

Keywords:
Metabolomics
BPA
MCF-7
Temporal profiling
Metabolic adaption
Dysregulation correlation

ABSTRACT

The biochemical consequences induced by xenobiotic stress are featured in dose-response and time-resolved landscapes. Understanding the dynamic process of cellular adaptations is crucial in conducting the risk assessment for chemical exposure. As one of the most phenotype-related omics, metabolome in response to environmental stress can vary from seconds to days. Up to now, very few dynamic metabolomics studies have been conducted to provide time-dependent mechanistic interpretations in understanding xenobiotics-induced cellular adaptations. This study aims to explore the time-resolved metabolite dysregulation manner and dynamically perturbed biological functions in MCF-7 cells exposed to bisphenol A (BPA), a well-known endocrine-disrupting chemical. By sampling at 11 time points from several minutes to hours, thirty seven significantly dysregulated metabolites were identified, ranging from amino acids, fatty acids, carboxylic acids and nucleoside phosphate compounds. The metabolites in different pathways basically showed distinct time-resolved changing patterns, while those within the common class or same pathways showed similar and synchronized dysregulation behaviors. The pathway enrichment analysis suggested that purine metabolism, pyrimidine metabolism, aminoacyl-tRNA biosynthesis as well as glutamine/glutamate (GABA) metabolism pathways were heavily disturbed. As exposure event continued, MCF-7 cells went through multiple sequential metabolic adaptations from cell proliferation to energy metabolism, which indicated an enhancing cellular requirement for elevated energy homeostasis, oxidative stress response and ER-α mediated cell growth. We further focused on the time-dependent metabolite dysregulation behavior in purine and pyrimidine metabolism, and identified the impaired glycolysis and oxidative phosphorylation by redox imbalance. Lastly, we established a restricted cubic spline-based model to fit and predict metabolite's full range dysregulation cartography, with metabolite' sensitivity comparisons retrieved and novel biomarkers suggested. Overall, the results indicated that 8 h BPA exposure leaded to global dynamic metabolome adaptions including amino acid, nucleoside and sugar metabolism disorders, and the dysregulated metabolites with interfered pathways at different stages are of significant temporal distinctions.

✉ Corresponding author
E-mail: mlfang@ntu.edu.sg

Special Issue—Frontier Progresses from Chinese-American Professors of Environmental Engineering and Science (Responsible Editors: Xing Xie, Jinkai Xue & Hongliang Zhang)

1 Introduction

Biological systems are highly refined processes subject to dynamic metabolism regulation (Chen et al., 2012; Link et al., 2015). Being the terminal products of transcriptomic and proteomic activities, intercellular metabolites' change in response to metabolic syndrome factors can vary from seconds to days (Yanes et al., 2010; Jain et al., 2012; Link et al., 2013). Given that metabolites are among the most phenotype-relevant cellular components under environmental stress (Moreno-Sánchez et al, 2008), dynamic metabolomics study exhibits its advantages in characterizing the real-time metabolome dysregulation pattern both comprehensively and comparatively (Guo et al., 2022; Wu et al., 2022). Although techniques like quantitative metabolic flux provides a promising perspective for time-dependent omics exploration, acquisition of high-quality dynamic metabolomics data remains challenging in regard to non-invasive *in situ* sampling, improper labeling, insufficient model options and intensive workload (Zamboni et al, 2009; Link et al., 2015; Tugizimana et al., 2019). Time-resolved metabolomics, acting as an indispensable compartment under dynamic metabolomics framework, plays an important role in providing unbiased information about mechanisms of metabolic disorders, guidance on drug development and prognostic advice (Spégel et al, 2013; Kowalski et al., 2015; Geng et al., 2016; Krycer et al., 2017; Halama et al., 2019; Lu et al., 2020). Hannes et al. constructed a time-of-flight mass spectrometry (TOF-MS) auto-sampling system which enables bacteria's metabolome real-time monitoring (Link et al., 2015), and observed an inhibition effect of nucleotide synthesis under starvation which suggested salvage pathway is preferred than *de novo* for less energy consumption. Lee et al. investigated multiple metabolic response alterations along cell's canceration procedure, including upregulation of nucleotide biosynthesis, downregulation of oxidative phosphorylation and epigenome maintenance breakdown (Lee et al., 2017). In practice, researchers have allocated antimalaria drug's performance from time-resolved metabolomics study, to achieve the mode of action determination as well as pharmacokinetics optimization (Allman et al., 2016; Cobbold et al., 2016; Cobbold and McConville, 2019).

As time-resolved metabolomics being utilized as a potential tool, new challenges have been posed by the annotation and information extraction from the massive amount of dynamic omics data generated (Liang et al., 2020). Up to date, various solutions have been established to parameterize the time-resolved metabolomics, furtherly to interpret the underlying biological principles (Zampieri et al., 2017). Zak et al. developed a supervised machine-learning based protocol to unbiasedly predict time-series metabolic pathway dynamics, which proves a supreme performance compared with traditional Michaelis–Menten kinetics fitting (Costello and Martin, 2018). Nyamundanda et al. proposed an automated regression algorithm to identify biomarkers with time-resolved dysregulation importance (Nyamundanda et al., 2014). On top of that, researchers are paying increasing attention on multi-omics informatics development, ranging from tensor factorizations, smooths, mean-variation-weighted, and dimension-reducing principal component analysis, etc. (Smilde et al., 2010; Zhang et al., 2015; Li et al., 2021). Though ambiguities and false positive conclusion reached occasionally, the generated algorithm along with prediction models have brought novel and promising insights into the underlying correlation of metabolic features with disease status and prognostic impacts regarding time influence (Zhang et al., 2015; Zeng et al., 2022). However, very few studies are concerned with environmental factors' contributions through time-resolved metabolomics. Furthermore, one knowledge gap to fill is the derivation of chemical exposure's metabolic toxicokinetics and extrapolation modelling from time-series metabolomics data consequently (Fu et al., 2021; Liu et al., 2021; Luan et al., 2021).

Bisphenol A (BPA), an endocrine disrupting chemical of great public health concern, is an ideal model compound of toxicological research interest due to its multiple molecular targets (Chen et al., 2014; Howdeshell et al., 1999). Sufficient evidence has demonstrated BPA's estradiol-mimic effect which induces pleiotropic toxicity by affecting endocrine, immune and reproduction system (Alonso-Magdalena, et al., 2006;Alonso-Magdalena et al., 2012; Engin and Engin, 2021). In our recent study, multi-omics research has reported BPA exposure with consequences on metabolic pathways perturbation including glycolysis, purine metabolism, tricarboxylic acid cycle with a clear dose-response dependence (Yue et al., 2019; Jia et al., 2022; Zhao et al., 2022). Yet, no previous research has adopted time-resolved metabolome strategies to carry out BPA's dynamic hazard identification and risk assessment.

Here, we adopted time-resolved untargeted metabolomics to characterized global temporal metabolite profiles during 8 h BPA exposure. The dysregulated metabolites and interfered pathways were firstly identified, with the biochemical mechanisms interpreted. We further detailed the time-resolved metabolism patterns with distinct predominant pathways derived on each stage, and observed significant metabolic transitions which related to varying cellular event requirements. Furthermore, the fitting models of dysregulated metabolites within application domain are established, to provide a solid real-time full range prediction of metabolite dysregulation, as well as an insight into the relative sensitivity extrapolation and novel biomarkers discovery. Collectively, this dynamic metabolomics study demonstrated a unique time-resolved metabolome

dysregulation behavior and explored the distinct metabolic adaptions due to temporal cell function emphasis.

2 Materials and methods

2.1 Cell Culture and reagent preparation

MCF-7 cell line was purchased from the American Type Culture Collection. Cells were kept in liquid nitrogen vapor phase until reviving. After reviving, cells were maintained in humidified 37 °C atmosphere containing 5 % CO_2. Dulbecco's modified eagle medium (DMEM; supplemented with additional glucose, fetal bovine serum, L-glutamine and sodium pyruvate as instructed) was applied as the growth medium. BPA used for cell treatment was purchased from Sigma-Aldrich, with stock solution (20 mmol/L) prepared in dimethyl sulfoxide (DMSO, 99.8 %). All of the analytical reagents applied in this study are of high-performance liquid chromatograph grade or higher unless otherwise stated.

2.2 BPA exposure and metabolite extraction

MCF-7 cells were seeded in 6-well plates with starting density of 0.4×10^6 for each well. When they reached about 80 % confluency, the cells were exposed to BPA with final concentration of a fixed 100 μmol/L at ten varying time points (each time point with four biological replicates). The selection of this concentration was based on our previous study and most metabolic dysregulation yet no obvious toxicity has been observed (Aghajanpour-Mir et al., 2016; Zhao et al., 2021). Cells (n = 4 replicates for each) after treatment with duration of 0.25 h, 0.5 h, 0.75 h, 1 h, 1.5 h, 2 h, 3 h, 4 h, 6 h, and 8 h, respectively were quickly quenched and stored in –80 °C fridge (one sample at 1 h was lost due to centrifuge operations). As reported previously, the doubling time for MCF-7 proliferation ranges from 31.2 h to 80 h (Sweeney et al., 1998; Jain et al., 2012; Cowley et al., 2014). It can be derived that the theoretically maximum proliferation rate falls around 7 %–18 % at t = 8 h, which is supported by our preliminary survival test (Fig. S2). Taking cell cycle, observable outcome and nutrient limit into consideration, we finally decided to use 8 h as final exposure point. As expected, the effect of undulated cell counts at each time point have been treated as marginal and negligible.

Control samples (n = 3) were prepared by quenching the cells instantly after BPA was added into the system. Metabolite extraction protocol was modified based on our previous studies (Fang et al., 2015; Beyer et al., 2018; Liu et al., 2020; Zhao et al., 2021). After rinsing with PBS twice rapidly, metabolites were collected with 1.6 mL ice-cold methanol: acetonitrile: water (2:2:1, v/v/v) and harvested by a cell scraper. To preserve and extract the pure metabolite, freeze-thaw steps were conducted thrice using liquid nitrogen followed by sonication in an ice bath for 10 min. After placed at –40 °C for 1 h, the samples were violently vortexed and centrifuged for 15-min at a speed of 13000 r/min at 4 °C to precipitate proteins. The supernatant was collected and evaporated to almost dryness by a CentriVap centrifugal vacuum concentrator (Labconco, USA). The resulting extracts were then reconstituted by 100 μL acetonitrile: water (1:1, v/v), sonicated on ice for 10 min, and centrifuged for 15 min at 13000 r/min and 4 °C to remove insoluble debris. The final metabolite products were transferred to HPLC vials with insert and stored at –40 °C for further instrumental analysis (Xu et al., 2020; Xu et al., 2021).

2.3 Metabolite profiling and QA/QC

Instrumental analysis was performed on High-performance Liquid Chromatography (HPLC) system coupled with Quadrupole Time-of-Flight (QTOF) mass spectrometer. Details of the profiling method was a modified version from our previous study (Fang et al., 2015; Beyer et al., 2018; Zhao et al., 2022). In our previous study, most of the altered metabolites were shown in the HILIC negative mode (ESI-), and thus we only used this method due to the large number of samples analyzed. For instrumental analysis, the analyzed components were separated by UPLC (Ultra performance liquid chromatography) Acquity BEH amide column (1.7 μm, 2.1 mm × 100 mm), with a running time of 12.5 min per sample. Briefly, mobile phase A was 25 mmol/L NH_4OH with 25 mmol/L NH_4OAc in water, and mobile phase B was acetonitrile. Mobile phase linear gradient as well as other parameters were set as previously reported (Zhao et al., 2022). To correct mass accuracy, retention time shift and response drift, a mixture consists of all samples (QC sample) was prepared by pooling all treated and control cell samples. QC analysis was conducted by injecting a QC sample and a blank sample (acetonitrile: water, 1:1, v/v) once among every eight injections of biological samples. Data-dependent acquisition and targeted MS/MS of selected precursors were also run on the QC sample for metabolite identification purposes (Xu et al., 2021b).

2.4 Metabolite identification, metabolic pathway analysis and data visualization

The metabolite profiling data (MS1 full scan) were processed with Agilent Masshunter Acquisition Software 6.0 and further analyzed on cloud-based XCMS Online platform (Smith et al, 2006). 11 groups of time-dependent MS1 profiling data were analyzed through multigroup analysis. Briefly, after peak picking, alignment and annotation, the candidature features were firstly screened with principles listed: signal-to noise (S/N) ratio > 10,

maximal intensity > 10000, |fold change| ⩾ 1.1, to obtain the dysregulated metabolites with significant biological meaning. To compare the metabolite changes at various time points, one-way *ANOVA* along with *Duncan post-hoc* analysis was applied to examine whether the treatment group is statistically different; an FDR-adjusted *p*-value ⩽ 0.05 was considered statistically significant. After filtering out the insignificantly dysregulated metabolic features, metabolite identification was carried out using a few filters including accurate mass match, MS/MS fragment match (auto/targeted MS/MS) and in-house retention time match (Zhao et al., 2021). Additionally, metabolite features were searched against several open-source platforms, including METLIN (Smith et al., 2005), KEGG and HMDB databases.

Metabolic Pathway Enrichment Analysis were conducted using Metaboanalyst and Metamapp with data at 8 h point. The calculated nodes and edges were extracted and visualized by Cytoscape. To characterized time-resolved metabolites' dysregulation tendency and interspecies correlation, restricted cubic spline fitting (RCS) modelling was applied as previously stressed (Inoue et al., 2020; Johannesen et al., 2020). Other data visualization such as heatmap, principal component analysis, rose diagram and correlation plot were completed using R-studio (version 4.0.1) (Vienna, Austria) and GraphPad Prism (version 7), while statistical analyses were performed by SPSS Statistics (version 22). All data were processed and optimized in advance (log-transformed, FDR-adjusted normalized, Pareto scaling, etc.) as suggested in the workflow summarized in (Fig. 1).

3 Results and discussion

3.1 Metabolomics profiling

To uncover the metabolites of time-dependent dysregulation interest, we conducted untargeted metabolomics analysis by initiating with semi-quantitatively aligning the features across all samples and conducting the multiple group analysis. In total, 6143 significant features were identified with FDR-adjusted *p*-value ⩽ 0.05 calculated by one-way *ANOVA*. Overall, a positive correlation was observed between exposure time with significant feature numbers (Fig. 2C), and the upregulated features were ubiquitously outnumbered than the downregulated ones. PCA analysis exhibits quite well grouping pattern (Fig. 2A), and the percentage of explained variances reaches approximately 33.6 % and 19.9 % for the first two components respectively, (Fig. 2B), which suggests a characteristic distinction for the time-resolved metabolome change.

We also summarized the overlapping and distinct features at 2 h, 4 h, 6 h and 8 h in a *Venn* diagram (Fig. 2D). Among all treatment groups, the overlapped percentage for dysregulated features were significantly distinct (72.9 % for t =2 h, 64.7 % for t =4 h, 79.5 % for t = 6 h and 76.5 % for t= 8 h, respectively). The coverage discrepancy may imply certain intrinsic relationships between features' alteration tendency as exposure time increasing.

3.2 Dysregulated metabolite identification

Based on the feature alignment and annotation results, we manually curated the shifted *m/z* and retention time. Combined with in-house standard library matching and MS/MS fragmentation validation, 37 significantly dysregulated metabolites were confidently identified at either level 1 confirmed structure or level 2 probable structure (Schymanski et al., 2014), ranging from amino acids, fatty acids, carboxylic acids and nucleoside phosphate compounds (Table S1). Hierarchical clustering heatmap of 37 metabolites was presented in (Fig. 3). The clustering pattern exhibits quite reasonable dynamically-distinct features, as well as the simultaneous/ synchronized dysregulation characteristic for certain metabolites within one shared category, which is consistent with our previous report (Zhao et al., 2022).

Based on the clustering, a few featured patterns can be observed. For one thing, different metabolites exhibited distinct temporal dysregulation patterns. Among all the identified metabolites, lactic acid showed the highest fold change (FC = 4.0) at 8 h, while citraconic acid hits the minimum (FC = 0.1) at 6 h. The intercellular accumulation of lactic acid implied an enhanced glucose uptake due to Warburg effect (Brodsky et al., 2019). Several metabolites were significantly upregulated to certain degree after 8 h exposure (NADH, N-Acetylglutamic acid, lactic acid, CDP-ethanolamine, etc.), while others exhibited a monotonic downregulation tendency (glutamic acid, phosphocreatine, pyroglutamic acid, etc.), which is consistent with previous studies (Potratz et al., 2017; Liu et al., 2020; Zhao et al., 2022). The decrease of glucose and phosphocreatine indicated a higher metabolic requirement for sugar and energy consumption, which suggests BPA exposure induced disturbances in TCA cycle and glycolysis (Azevedo et al., 2019). It is also worthy to note that a few metabolites were behaving a global oscillation behavior. For example, UDP-glucose plays indispensable roles in polysaccharides biosynthesis by gluconeogenesis and glycogen metabolism, also extracellular signalling as inflammatory responses (Zimmer et al., 2021), which suggested a multi-factor and crossed-pathway co-regulation manner (Kerkhofs et al., 2020).

On top of that, similar or synchronized dysregulation patterns were observed for certain metabolites within one common class, which implies a certain intercorrelated dysregulation principle. For example, the dysregulation pattern for amino acids (leucine, lysine, proline, tyrosine, valine) as well as nucleotide triphosphates (ATP, GTP,

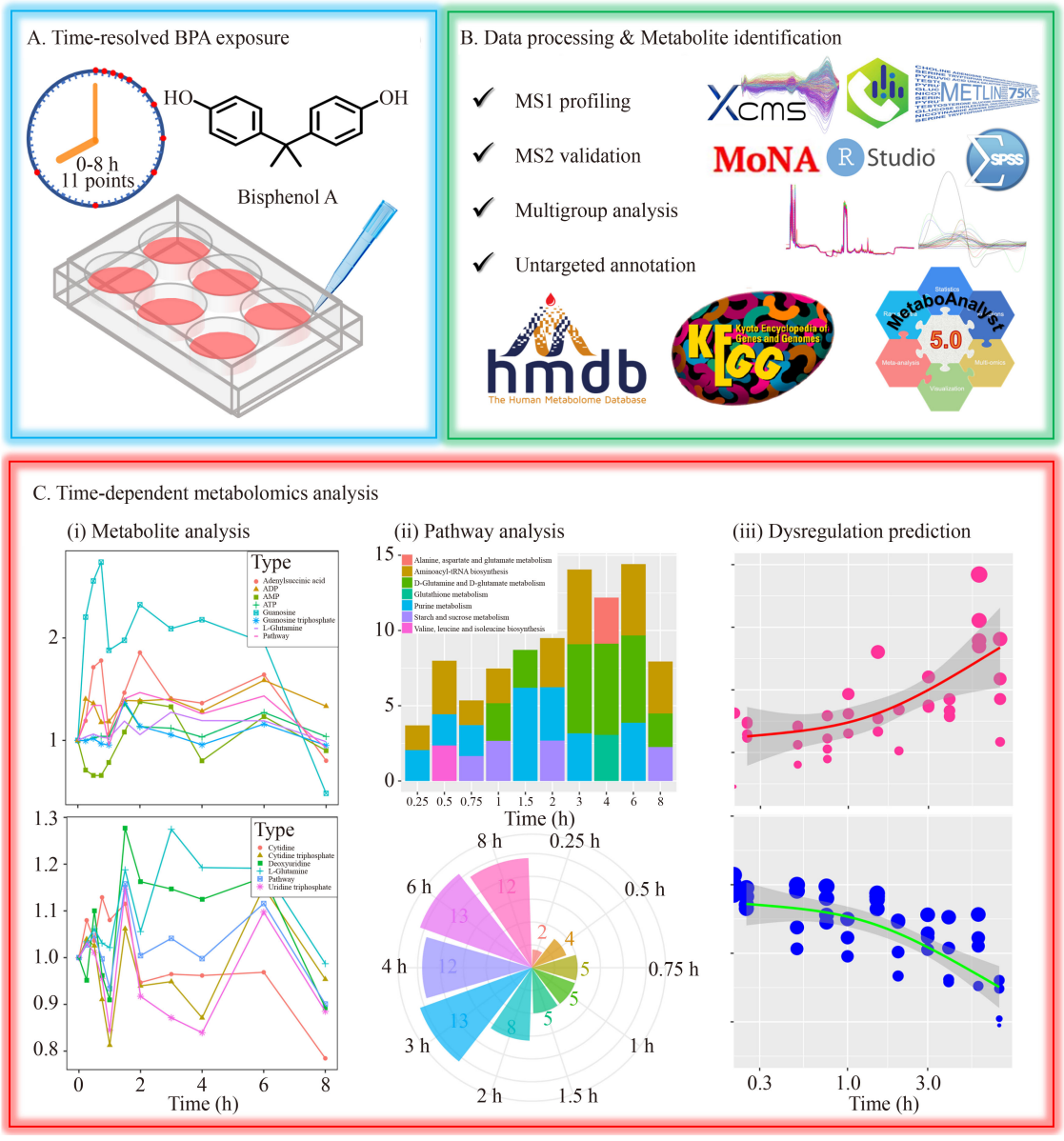

Fig. 1 Tiered approach of the time-resolved metabolomics study. (A) Experimental workflow to harvest MCF-7 cells exposed to Bisphenol A at 11 varying time points (0 h, 0.25 h, 0.5 h, 0.75 h, 1 h, 1.5 h, 2 h, 3 h, 4 h, 6 h, and 8 h), with intercellular metabolites extracted and analyzed by HPLC-MS. (B) Data processing and metabolite identification under untargeted metabolomics framework. The applied methodology included but not limited to: MS1 profiling, MS2 validation, RT shifted correction, in-house standard library alignment, one-way *ANOVA*, *t*-test, pathway enrichment analysis, etc. (C) Time-resolved metabolomics was implemented to uncover metabolite time-dependent dysregulation behavior, including metabolite dysregulation analysis, temporal pathway enrichment and restricted cubic spline-based prediction.

CTP, UTP). The dysregulated amino acids play important roles in the promotion of energy metabolism, protein biosynthesis, hormone production and inhibition of proteindegradation(Slominski et al., 2012; Acevedo et al., 2013; Duan et al., 2016). In addition, the disturbed nucleotide triphosphates were explicitly related to purine/pyrimidine metabolism dysfunction (Liu et al., 2020), cell cycle maintenance, as well as potentially linked to BPA provoked DNA damage and degradation. The differences of metabolomic effect between exposure time could be partially explained by the gradient increasing estrogenic activity (Zhao et al., 2022). Overall, the time-dependent regulation of amino acids, nucleosides and sugar suggested global metabolome disturbances, as a consequence from environment estrogen exposure and concomitant ERα-mediated induction of cell proliferation (Potratz et al., 2017). Collectively, the continuing BPA exposure triggered significant time-resolved metabolome changes for various metabolites.

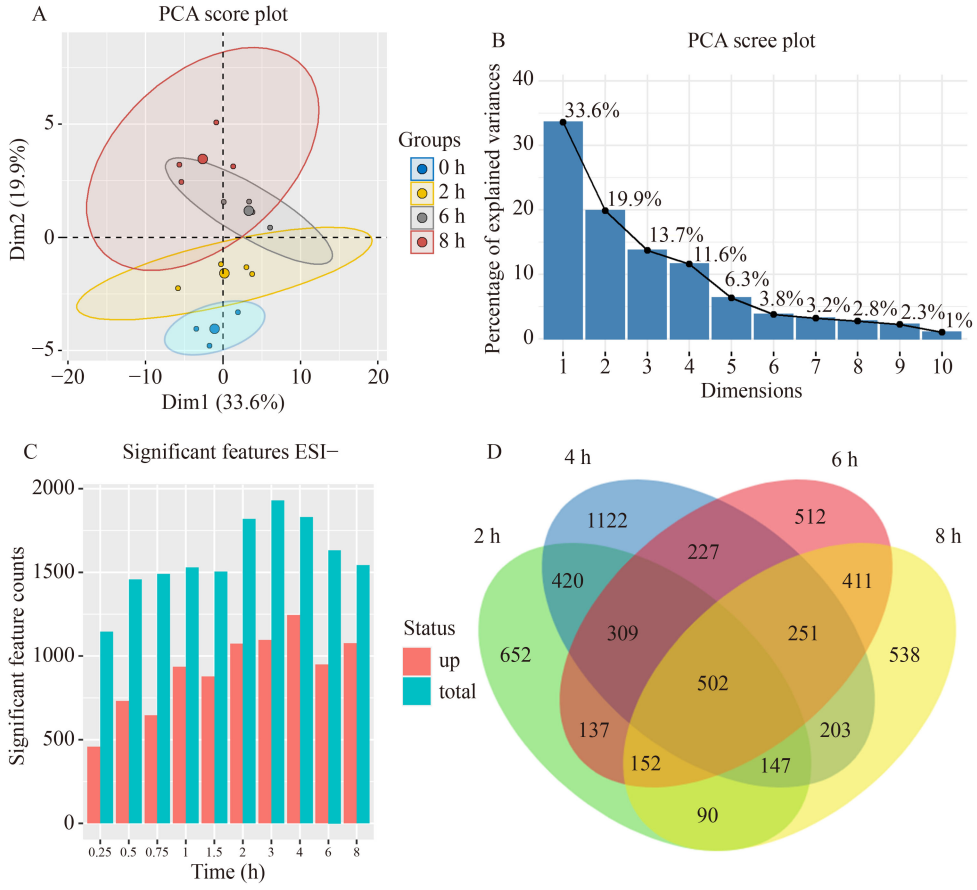

Fig. 2 (A) Principal component analysis score plot of aligned features at 0 h, 2 h, 6 h, and 8 h (3 control samples and 1 mean point at 0 h; 4 treated samples and 1 mean point at 2 h, 6 h, and 8 h); (B) Principal component analysis scree plot of total ion features at 0 h, 2 h, 6 h, and 8 h; (C) Up and down-regulated significant features of 10 time point detected by global profiling (pairwise comparison with control samples); (D) Venn diagram summarizing the number of shared and distinct features of total metabolome features at 2 h, 4 h, 6 h, and 8 h (multigroup analysis).

3.3 Time-series metabolomic pathway analysis

Metabolomic pathway analysis was further conducted by pathway enrichment of the dysregulated metabolites. The top interfered pathways within 8 h exposure were purine metabolism, pyrimidine metabolism, aminoacyl-tRNA biosynthesis as well as glutamine/glutamate metabolism (Fig. 4A). The result is also in line with several earlier studies suggesting that exposure to developmental toxicants such as BPA can induce disturbances in arginine metabolism, glutamate metabolism and citrate cycle (West et al., 2010; Zhao et al., 2021). The perturbation of aminoacyl-tRNA biosynthesis was also supported by earlier studies which observed an increase in amino acid concentrations in BPA treated-embryos (Huang et al., 2017; Ortiz-Villanueva et al., 2017). What is more, nucleotide phosphate levels were elevated through both *de novo* synthesis (glutathione) (Yuan et al., 2016; Fan et al., 2020) and salvage pathway (Vahdati Hassani et al., 2018) as reported. Other pathways include amino sugar and nucleotide sugar metabolism, galactose metabolism and TCA cycle indicated an upregulation of glucose oxidation reactions, elevated levels of proteolytic metabolism and energy consumption (Liu et al., 2020). In total, the enriched pathways revealed an enhancing proliferation trend for MCF-7 cells through BPA's estrogenic effect, with multi-pathway and multi-ending adverse effects involving global amino acid, glucose and lipid metabolism dysfunctions. Compared to previous studies (24–48 h *in vitro*), this study demonstrates that short-term exposure to BPA can lead to similar and observable disorders in varieties of primary metabolites and metabolism intermediates.

On top of that, we further specified the time-series regulatory patterns for certain pathways, in order to specifically describe the dynamic changes of selected biological processes with reference to exposure time. To demonstrate the featured pathway during 8-h BPA exposure, we identified the top 3 mostly enriched pathway at each time point (Fig. 4B). From 0.25 h to 2 h, purine metabolism features the most dominant regulating pathway, which indicated a temporal metabolic emphasis on one-carbon unit biosynthesis and tumor cell proliferation (Yin et al., 2018). The enriched upregulation

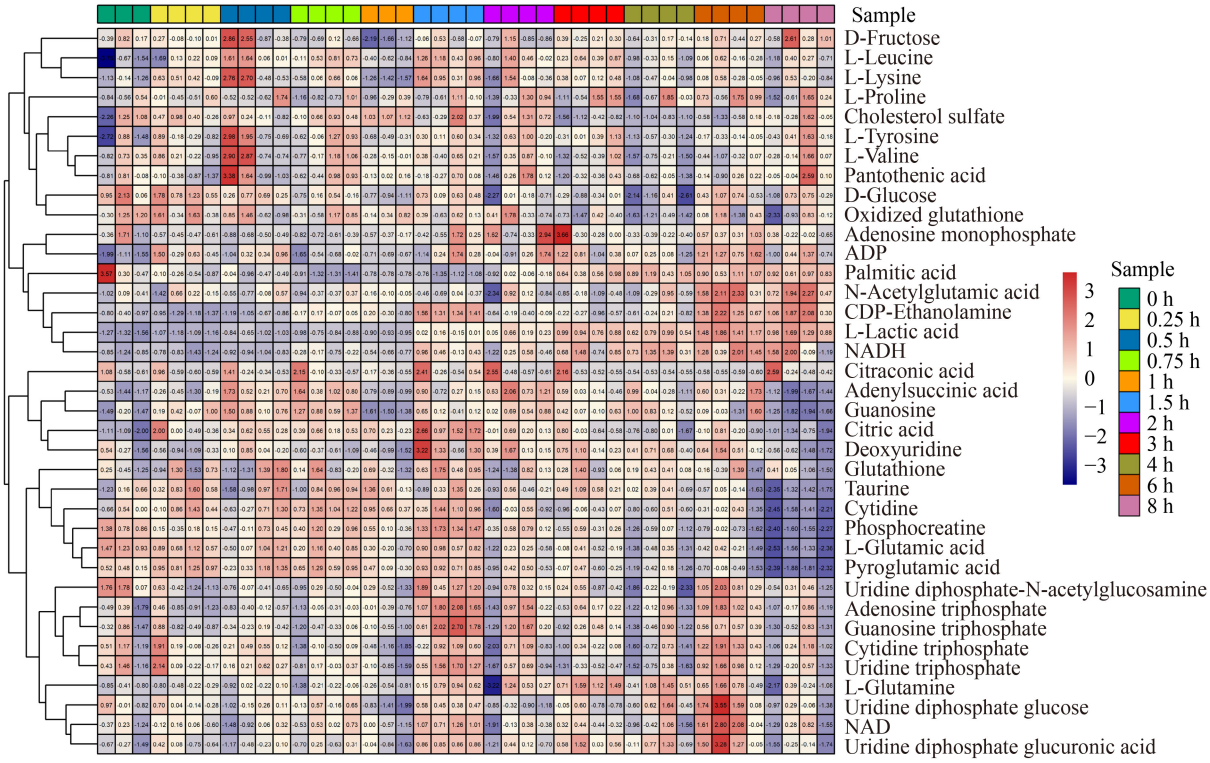

Fig. 3 Clustered heatmap of 37 significant dysregulated metabolites. Scales in colored key represent z-score scaled fold change value of metabolites. [Abbreviations: Nicotinamide adenine dinucleotide (NAD); 1,4-Dihydronicotinamide adenine dinucleotide (NADH); Adenosine 5'-diphosphate (ADP).]

of nucleotide phosphates (AMP, ADP, ATP) was greatly attributed to enhanced *de novo* purine biosynthesis (Lv et al., 2020), as well as the blockage in nucleotides degradation consequently (Xu et al., 2021). From 2 h to 6 h, glutamate/ glutamine metabolism showed the top enrichment, which suggested a metabolic alteration to meet elevated energy requirements. Glutamine is an essential component in ATP biosynthesis, which fuels TCA cycle and nitrogen metabolism (Mazat and Ransac, 2019). Its upregulation suggested a higher intercellular energy demand from enhanced sugar metabolism after 2 h BPA exposure. The observed metabolic adaption from cell growth to energy metabolism interpreted the intercellular metabolic adaptions due to temporal cell function requirements, which is of great significance in understanding BPA's toxicology mode of action, as well as providing an insight about the time-resolved biochemical hazard identification (Kalkhof et al., 2015).

We further managed to plot the average abundance profiles of detected metabolites within four pathways individually (Fig. 4D), which showed tangible distinctions mutually. The rose diagram showed the number of significantly affected metabolites as well as pathways soared with lasting exposure time, and the metabolic disruption severity continuously increased (Fig. 4C). Overall, the results suggested that multiple pathways were distinctly activated or inhibited with reference to time. Time-resolved changes in metabolic pathway profiles were achieved through co-regulation of various metabolites (Metallo and Vander Heiden, 2013).

3.4 Time-resolved metabolite dysregulation pattern spotlight

To accurately describe the time-response relationship of metabolites and investigate the time-induced microscale effects on biological functions, we further focused on the metabolites in purine metabolism and pyrimidine metabolism pathways (Fig. 5**)** as they were comparably abundant and globally pathway-enriched. As the primary catabolism compartment for intercellular signalling, energy transfer and DNA/RNA production, purine and pyrimidine metabolism are among the rapidest responding biological processes dealing with xenobiotic exposure (Liu et al., 2020). ATP is the basic cellular fuel component, whose dysregulation pattern shows an increasing energy consumption demand. AMP is a crucial composition for coenzyme (CoA, NAD, etc.), from which we inferred an enhancing oxidative phosphorylation and cellular respiration. UTP acts as the energy source for glucose/ galactose metabolism, and CTP involves energy transfer in membrane lipid metabolism. The time-resolved regulation of the mentioned purine/pyrimidine nucleotides showed a global elevated energy homeostasis,

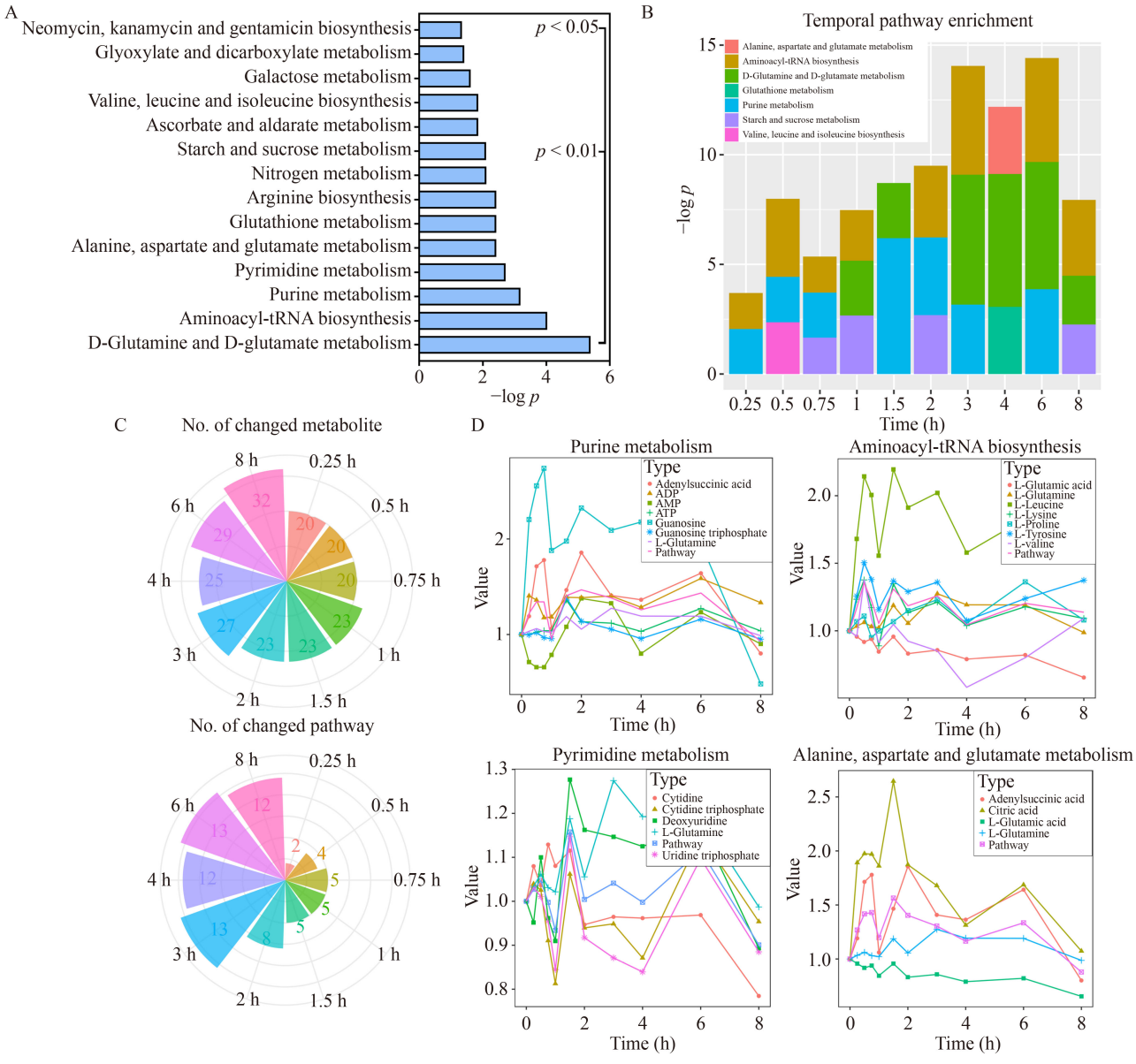

Fig. 4 (A) Metabolite enrichment analysis of 37 significant dysregulated metabolites ($p \leqslant 0.05$); (B) Temporal diagram of the top 3 mostly enriched pathway (with minimum p-value) at each time point; (C) Rose diagrams which present the number of significantly changed metabolites and significantly disturbed pathway ($p \leqslant 0.05$) at each time point; (D) Average abundance profiles of detected metabolites for four pathways (purine metabolism, pyrimidine metabolism, aminoacyl-tRNA biosynthesis, alanine, aspartate and glutamate metabolism). The pathway value was set as the mean of the involved metabolite within specified pathway. All abundance levels are normalized to their mean values at 0 h.

which may be related to membrane lipid biosynthesis, protein glycosylation and upregulated cell cycle progression (Moffatt and Ashihara, 2002; Quéméneur et al, 2003; Liu et al., 2020). This is reasonable as MCF-7 is a hormone-sensitive cell line, for which BPA can induce environmental estrogenic effects (Blom et al., 1998; Gould et al., 1998). Another evidence is that the oxidized-glutathione and glutathione metabolism dysfunction indicated an increasing oxidative stress that cells experience. This is consistent with multiple studies suggesting BPA exposure has led to depression of several antioxidant enzymes, including glutathione reductase and glutathione peroxidase (Meli et al., 2020). Besides, tumor cells often tend to enhance glycolysis with extra ATP produced, as a protection against the inflammatory damage from xenobiotic intrusion (Brand and Hermfisse, 1997). And it is validated by an earlier trans-omics study which reported plenty of inflammatory-related genes along the Nrf2-ARE pathway were substantially expressed in MCF-7 cells undergoing BPA exposure (Liu et al., 2020).

To prove this, we focused on two pairs of metabolites:

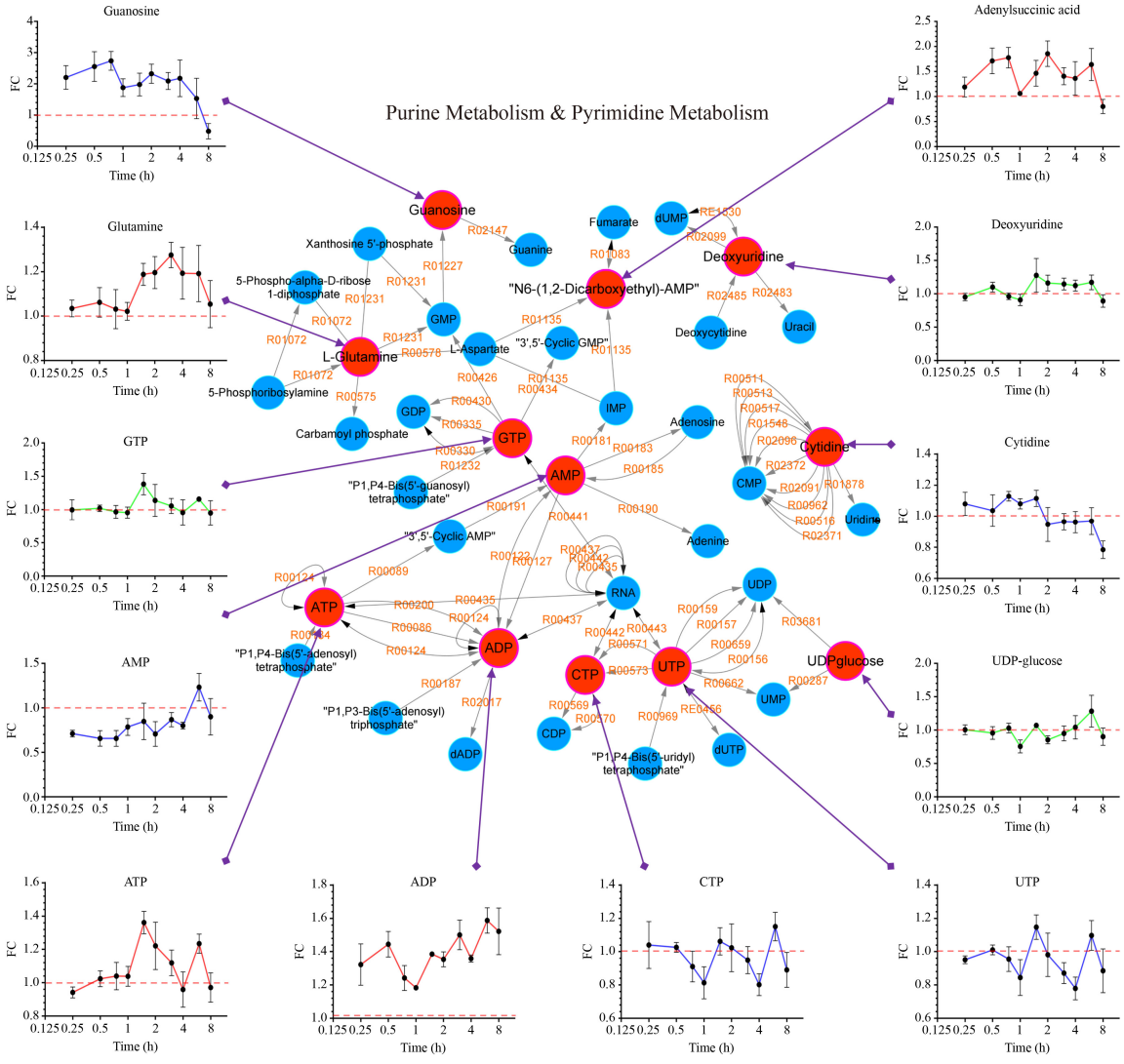

Fig. 5 Metabolomic analysis of purine metabolism and pyrimidine metabolism. The time-response plot for detected metabolites were shown (fold change *vs.* time), with red dashed line stands for control (FC = 1).

NAD with NADH, and glutathione (GSH) with oxidized GSH (GSSG) to check the intercellular oxidative stress and redox metabolism status (Figs. 6B and 6C). NAD/NADH ratio maintains a redox balance in mitochondrial activity through the electron transport chain. The observed excess NADH is linked with reactive oxygen species (ROS) production by inhibiting pyruvate dehydrogenase complex, which leads to DNA/protein damage and various metabolic syndromes (Wu et al., 2016). GSH/GSSG ratio is another important indicator in the assessment of redox state and cellular antioxidant capacity (Owen and Butterfield, 2010). Unlike the monotonic drop in NAD/NADH ratio, the observed GSH/GSSG value showed an oscillating behavior. For 0.25 h to 2 h, GSH's elevation is potentially resulted from cell proliferation events (Wu et al., 2004), which may also be attributed to enhanced cellular oxidative stress resistance (Kennedy et al., 202020). This result suggested that cells were undergoing time-dependent increased cellular oxidative stress, which in turn resulted in oxidative phosphorylation and glycolysis dysfunctions (Moreira et al., 2016), which is supported by an earlier study indicating that BPA exposure induced malate-aspartate shuttle functioning disorders (aspartate aminotransferase, glutamate-aspartate transporter, etc.) to break the NADH balance in the mitochondrial respiration chain (Kunz et al., 2011).

3.5 Metabolite time-response model fitting

To investigate the intrinsic relationship between different metabolites' regulation patterns, the Pearson correlation matrix was adopted to explore the characteristic linear association (Fig. 6A). Most metabolites exhibited weak co-dysregulation dependencies, while several showed regional clustering features. For example, N-Acetylglutamic

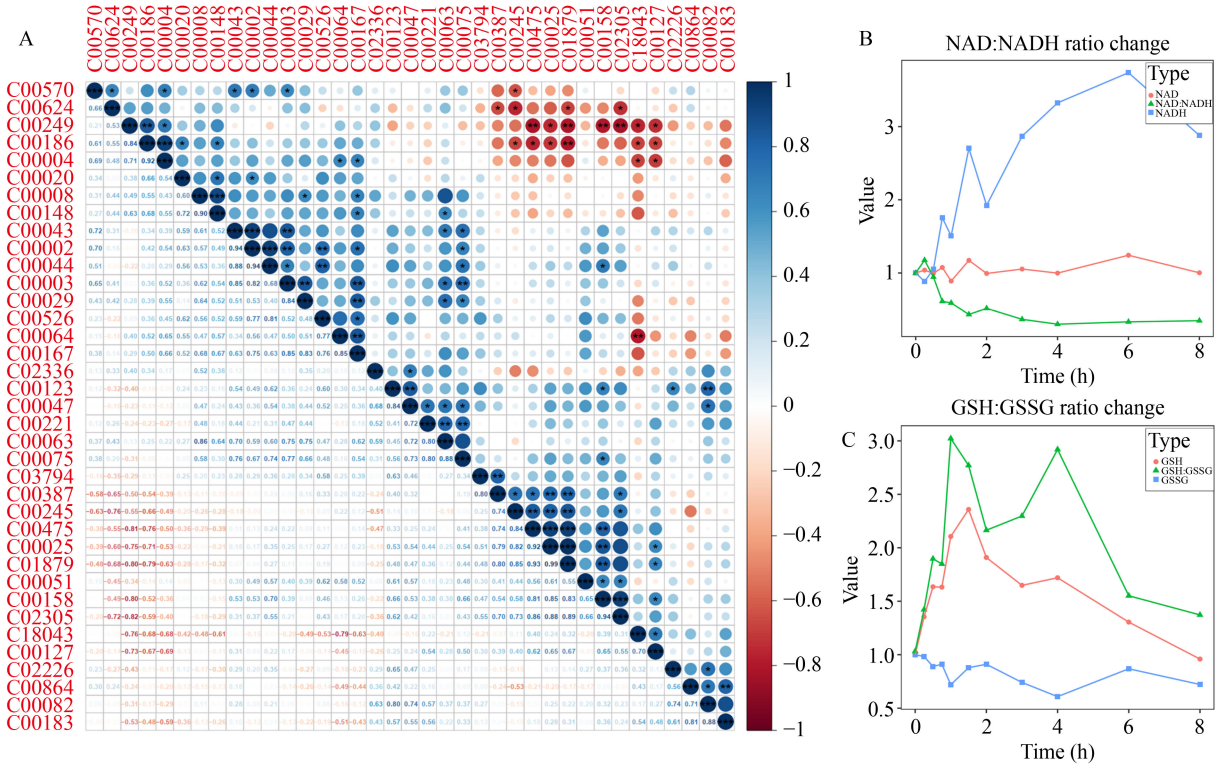

Fig. 6 (A) Pearson correlation matrix of 37 metabolites. Dots and figure in color stands for correlation coefficient from –1(red) to 1 (blue), with significance level presented ("*" for $p < 0.05$; "**" for $p < 0.01$; "***" for $p < 0.001$, respectively); (B) Schematic diagram of dynamically changing NAD:NADH ratio; (C) Schematic diagram of dynamically changing GSH:GSSG ratio.

acid (C00624) demonstrated quite positive regulation correlations with L-Glutamic acid (C00025), Pyroglutamic acid (C01879) and Citric acid (C00158). This is reasonable as the consumption and regeneration between glutamic acid and its derivatives maintains a dynamic balance from the GABA cycle to the TCA cycle (Petroff, 2007). Similarly, significant negative correlations were observed between UTP (C00075) with UDP-glucose (C00029) and UDPGA (C00043), which may suggest that BPA exposure triggered an enhanced conversion from UTP to UDP-glucose which fuels the TCA cycle as well as fulfills cell proliferation requirements (Kim et al., 2010). Scatterplots of fold changes at the adjacent time steps for 37 metabolites were further presented in Fig. S1. Typically, the metabolite changes between neighboring time points exhibit positive correlations, yet the dysregulation pattern and intensity vary between each period (Lee et al., 2017). The results also indicated a characteristic dysregulation rate for different metabolites, also the derivation of accurate and robust time-resolved models is essential for full-period cartography prediction.

To systematically evaluate the time-resolved dysregulation pattern for various metabolites, time-response relationships for each were fitted and several curves were presented (Fig. 7). Traditional monotonic dose-response methods can hardly be eligible for the time-resolved metabolism behavior characterization. Hereby, we implemented a restricted cubic spline fitting (RCS) protocol, as for its advantage in non-linearity continuous description and successful application in multiple public health issues (Desquilbet and Mariotti, 2010; Inoue et al., 2020; Johannesen et al., 2020). The established models not only provided an insightful tool to predict the metabolite dysregulation behavior in untested scenarios, also illustrate metabolites' relative sensitivity, which leads to novel biomarkers identification (Zhao et al., 2022). For example, the four presented metabolites (AMP, citrate, guanosine, glutamic acid) perform different biological functions in separate metabolic pathways. At 1 h, the predicted FC values for each are 0.75, 1.86, 2.28 and 0.9, respectively, which suggested metabolites' sequential relative sensitivity to BPA exposure (guanosine > citrate > AMP > glutamic acid). The information could further be adopted for potential biomarkers identification, for metabolites with higher dysregulation sensitivity (GTP, CTP, proline, etc.) (Zhao et al., 2022). The time-resolved dynamic metabolomics study shall provide insights into active metabolomics to construct a solid framework for elucidating metabolite real-time dysregulation pattern, which is also promising in the application of dynamic metabolome monitoring, prediction and extrapolation (Rinschen et al., 2019; Lai et al., 2021; Peng et al., 2022).

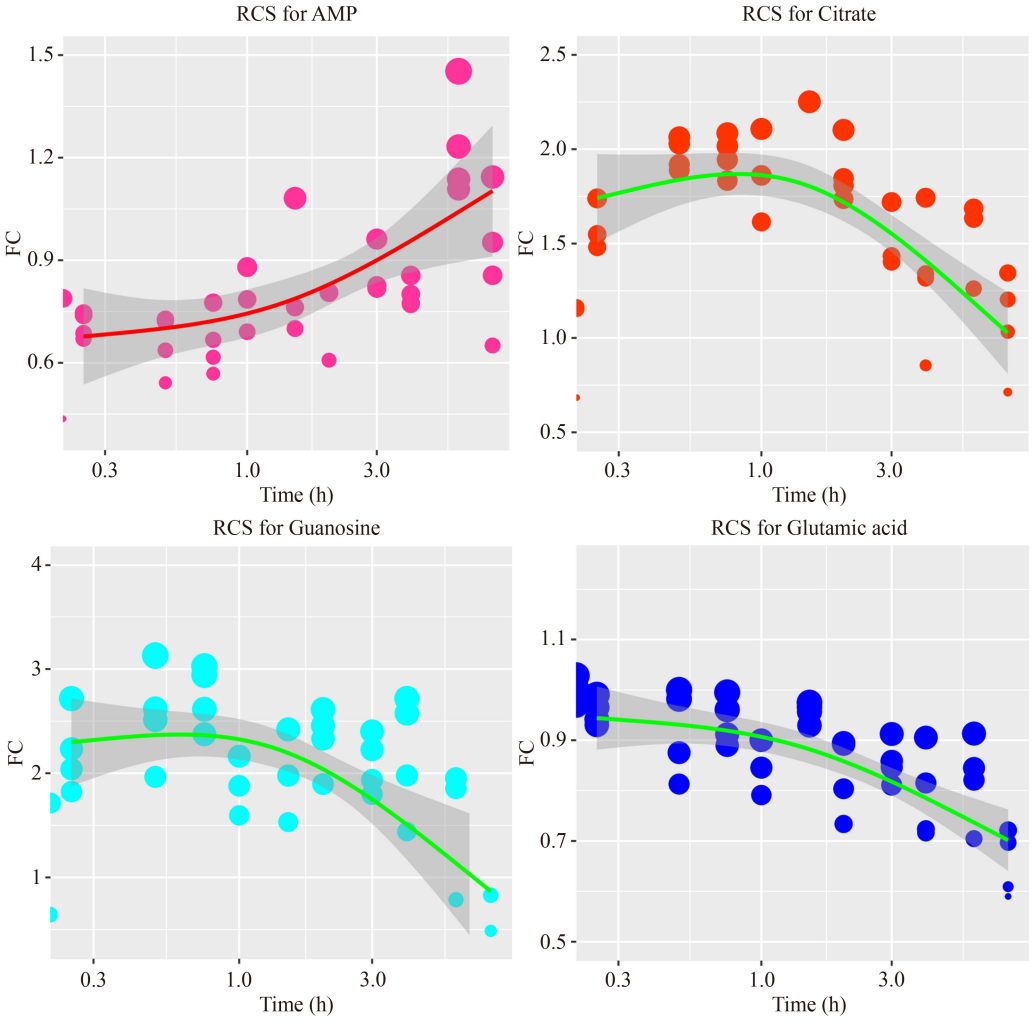

Fig. 7 Restricted cubic spline fitting curve of four metabolites, with confidence level indicated in grey ($p < 0.05$).

4 Conclusions

In summary, this study characterized the time-dependent cellular metabolome changes under BPA exposure. Thirty-seven significantly dysregulated metabolites were identified, ranging from amino acids, fatty acids, carboxylic acids and nucleoside phosphate compounds. Different metabolites basically showed distinct time-resolved changing patterns, while ones within common class showed similar and synchronized dysregulation manners. The pathway enrichment analysis suggested that purine metabolism, pyrimidine metabolism, aminoacyl-tRNA biosynthesis as well as glutamine/glutamate metabolism pathways were heavily disturbed. As exposure event lasting, MCF-7 cells went through clear sequential metabolic adaptions from cell proliferation to energy metabolism, which indicated an enhancing cellular requirement for elevated energy homeostasis, oxidative stress response and ER-α mediated cell growth. We further focused on the time-dependent metabolite dysregulation behavior in purine metabolism and pyrimidine metabolism, and identified the impaired glycolysis and oxidative phosphorylation by redox imbalance. Lastly, we established a restricted cubic spline-based model to fit and predict metabolite's full range dysregulation cartography, with metabolites' sensitivity comparisons retrieved and novel biomarkers suggested. Overall, the results indicated that 8 h BPA exposure leads to dynamic global metabolome adaptions including amino acid, nucleoside and sugar metabolism disorders, and the dysregulated metabolites with interfered pathways at different stages are of significant sequential distinctions. The major highlight of this pilot study is to explore a novel omics analytical technique which may be helpful in the depiction of dynamic metabolism cartography, as well as the induced adverse outcomes from a well-studied chemical exposure. Taken the quite short biological half-life of many environmental chemicals (within several hours) into consideration, this human-relevant study may inspire increasing research interests for the developments in chemical's hazard identification and risk assessment strategies.

Limitations of this study are further addressed as follows. As we investigated the metabolomic effect of BPA exposure within 8 h, the observed time-response dysregulation pattern may be incomplete. Also, the selection of time points isn't intensive enough to acquire real-time metabolome monitoring data, which may lead to key stages' neglections at which metabolic transition happens. *In vivo* and other *in vitro* models should also be adopted in future studies to validate the established time-response dysregulation models. The reached conclusion requires further validation, like chemical proteomics and flux studies. And the RCS modelling strategies can hardly be applied to all metabolites as some of them exhibit an oscillation dysregulation behavior. Overall, the time-resolved metabolomics study is promising for elucidation of the time-dependent metabolome dysregulation and identification of the sequential biochemical anomalies, yet still challenging in the interpretation of toxicological mechanisms, as well as the experiment's reproducibility and scalability.

Acknowledgements This work is supported by Singapore Ministry of Education Academic Research Fund Tier 1 (No. 04MNP000567C120) and Startup Grant of Fudan University (No. JIH 1829010Y).

Electronic Supplementary Material Supplementary material is available in the online version of this article at https://doi.org/10.1007/s11783-023-1604-5 and is accessible for authorized users.

References

Acevedo N, Davis B, Schaeberle C M, Sonnenschein C, Soto A M (2013). Perinatally administered bisphenol a as a potential mammary gland carcinogen in rats. Environmental Health Perspectives, 121(9): 1040–1046

Aghajanpour-Mir S M, Zabihi E, Akhavan-Niaki H, Keyhani E, Bagherizadeh I, Biglari S, Behjati F (2016). The genotoxic and cytotoxic effects of bisphenol-A (BPA) in MCF-7 cell line and amniocytes. International Journal of Molecular and Cellular Medicine, 5(1): 19–29

Allman E, Painter H, Samra J, Carrasquilla M, Llinás M (2016). Metabolomic profiling of the malaria box reveals antimalarial target pathways. Antimicrobial Agents and Chemotherapy, 60, AAC.01224–01216.

Alonso-Magdalena P, Morimoto S, Ripoll C, Fuentes E, Nadal A (2006). The estrogenic effect of bisphenol A disrupts pancreatic beta-cell function *in vivo* and induces insulin resistance. Environmental Health Perspectives, 114(1): 106–112

Alonso-Magdalena P, Ropero A B, Soriano S, García-Arévalo M, Ripoll C, Fuentes E, Quesada I, Nadal Á (2012). Bisphenol-A acts as a potent estrogen via non-classical estrogen triggered pathways. Molecular and Cellular Endocrinology, 355(2): 201–207

Azevedo L F, Porto Dechandt C R, Cristina de Souza Rocha C, Hornos Carneiro M F, Alberici L C, Barbosa F Jr (2019). Long-term exposure to bisphenol A or S promotes glucose intolerance and changes hepatic mitochondrial metabolism in male Wistar rats. Food and Chemical Toxicology, 132: 110694

Beyer B A, Fang M, Sadrian B, Montenegro-Burke J R, Plaisted W C, Kok B P C, Saez E, Kondo T, Siuzdak G, Lairson L L (2018). Metabolomics-based discovery of a metabolite that enhances oligodendrocyte maturation. Nature Chemical Biology, 14(1): 22–28

Blom A, Ekman E, Johannisson A, Norrgren L, Pesonen M (1998). Effects of xenoestrogenic environmental pollutants on the proliferation of a human breast cancer cell line (MCF-7). Archives of Environmental Contamination and Toxicology, 34(3): 306–310

Brand K A, Hermfisse U (1997). Aerobic glycolysis by proliferating cells: a protective strategy against reactive oxygen species. FASEB J, 11(5): 388–395

Brodsky A N, Odenwelder D C, Harcum S W (2019). High extracellular lactate causes reductive carboxylation in breast tissue cell lines grown under normoxic conditions. PLoS One, 14(6): e0213419

Chen M, Zhou K, Chen X, Qiao S, Hu Y, Xu B, Xu B, Han X, Tang R, Mao Z, Dong C, Wu D, Wang Y, Wang S, Zhou Z, Xia Y, Wang X (2014). Metabolomic analysis reveals metabolic changes caused by bisphenol-A in rats. Toxicological Sciences, 138(2): 256–267

Chen R, Mias G I, Li-Pook-Than J, Jiang L, Lam H Y, Chen R, Miriami E, Karczewski K J, Hariharan M, Dewey F E, et al. (2012). Personal omics profiling reveals dynamic molecular and medical phenotypes. Cell, 148(6): 1293–1307

Cobbold S, McConville M (2019). Determining the mode of action of antimalarial drugs using time-resolved lc-ms-based metabolite profiling. Methods in Molecular Biology, 1859: 225–239

Cobbold S A, Chua H H, Nijagal B, Creek D J, Ralph S A, McConville M J (2016). Metabolic dysregulation induced in plasmodium falciparum by dihydroartemisinin and other front-line antimalarial drugs. The Journal of Infectious Diseases, 213(2): 276–286

Costello Z, Martin H G (2018). A machine learning approach to predict metabolic pathway dynamics from time-series multiomics data. NPJ Systems Biology and Applications, 4(1): 19

Cowley G S, Weir B A, Vazquez F, Tamayo P, Scott J A, Rusin S, East-Seletsky A, Ali L D, Gerath W F, Pantel S E, et al. (2014). Parallel genome-scale loss of function screens in 216 cancer cell lines for the identification of context-specific genetic dependencies. Scientific Data, 1(1): 140035

Desquilbet L, Mariotti F (2010). Dose-response analyses using restricted cubic spline functions in public health research. Statistics in Medicine, 29(9): 1037–1057

Duan Y, Li F, Li Y, Tang Y, Kong X, Feng Z, Anthony T G, Watford M, Hou Y, Wu G, et al. (2016). The role of leucine and its metabolites in protein and energy metabolism. Amino Acids, 48(1): 41–51

Engin A B, Engin A (2021). The effect of environmental bisphenol-A exposure on breast cancer associated with obesity. Environmental Toxicology and Pharmacology, 81: 103544

Fan X, Hou T, Jia J, Tang K, Wei X, Wang Z (2020). Discrepant dose responses of bisphenol-A on oxidative stress and DNA methylation in grass carp ovary cells. Chemosphere, 248: 126110

Fang M, Ivanisevic J, Benton H P, Johnson C H, Patti G J, Hoang L T, Uritboonthai W, Kurczy M E, Siuzdak G (2015). Thermal degradation of small molecules: a global metabolomic

investigation. Analytical Chemistry, 87(21): 10935–10941

Fu Q, Scheidegger A, Laczko E, Hollender J (2021). Metabolomic profiling and toxicokinetics modeling to assess the effects of the pharmaceutical diclofenac in the aquatic invertebrate *Hyalella azteca*. Environmental Science & Technology, 55(12): 7920–7929

Geng S, Misra B B, Armas E, Huhman D V, Alborn H T, Sumner L W, Chen S (2016). Jasmonate-mediated stomatal closure under elevated CO_2 revealed by time-resolved metabolomics. Plant Journal, 88(6): 947–962

Gould J C, Leonard L S, Maness S C, Wagner B L, Conner K, Zacharewski T, Safe S, McDonnell D P, Gaido K W (1998). Bisphenol A interacts with the estrogen receptor alpha in a distinct manner from estradiol. Molecular and Cellular Endocrinology, 142(1–2): 203–214

Guo W, Shi Z, Zeng T, He Y, Cai Z, Zhang J (2022). Metabolic study of aristolochic acid I-exposed mice liver by atmospheric pressure matrix-assisted laser desorption/ionization mass spectrometry imaging and machine learning. Talanta, 241: 123261

Halama A, Aye M M, Dargham S R, Kulinski M, Suhre K, Atkin S L (2019). Metabolomics of dynamic changes in insulin resistance before and after exercise in PCOS. Frontiers in Endocrinology (Lausanne), 10: 116

Howdeshell K L, Hotchkiss A K, Thayer K A, Vandenbergh J G, vom Saal F S (1999). Exposure to bisphenol A advances puberty. Nature, 401(6755): 763–764

Huang S S Y, Benskin J P, Veldhoen N, Chandramouli B, Butler H, Helbing C C, Cosgrove J R (2017). A multi-omic approach to elucidate low-dose effects of xenobiotics in Zebrafish (Danio rerio) larvae. Aquatic Toxicology (Amsterdam, Netherlands), 182: 102–112

Inoue K, Ritz B, Brent G A, Ebrahimi R, Rhee C M, Leung A M (2020). Association of subclinical hypothyroidism and cardiovascular disease with mortality. JAMA Network Open, 3(2): e1920745

Jain M, Nilsson R, Sharma S, Madhusudhan N, Kitami T, Souza A L, Kafri R, Kirschner M W, Clish C B, Mootha V K (2012). Metabolite profiling identifies a key role for glycine in rapid cancer cell proliferation. Science, 336(6084): 1040–1044

Jia S, Li C, Fang M, Marques Dos Santos M, Snyder S A (2022). Non-targeted metabolomics revealing the effects of bisphenol analogues on human liver cancer cells. Chemosphere, 297: 134088

Johannesen C D L, Langsted A, Mortensen M B, Nordestgaard B G (2020). Association between low density lipoprotein and all cause and cause specific mortality in Denmark: prospective cohort study. BMJ (Clinical Research Ed.), 371: m4266

Kalkhof S, Dautel F, Loguercio S, Baumann S, Trump S, Jungnickel H, Otto W, Rudzok S, Potratz S, Luch A, Lehmann I, Beyer A, von Bergen M (2015). Pathway and time-resolved benzo[*a*]pyrene toxicity on Hepa1c1c7 cells at toxic and subtoxic exposure. Journal of Proteome Research, 14(1): 164–182

Kennedy L, Sandhu J K, Harper M E, Cuperlovic-Culf M (2020). Role of glutathione in cancer: from mechanisms to therapies. Biomolecules, 10(10): 1429

Kerkhofs M H P M, Haijes H A, Willemsen A M, van Gassen K L I, van der Ham M, Gerrits J, de Sain-van der Velden M G M, Prinsen H C M T, van Deutekom H W M, van Hasselt P M, Verhoeven-Duif N M, Jans J J M (2020). Cross-omics: integrating genomics with metabolomics in clinical diagnostics. Metabolites, 10(5): 206

Kim H, Choi J, Kim T, Lokanath N K, Ha S C, Suh S W, Hwang H Y, Kim K K (2010). Structural basis for the reaction mechanism of UDP-glucose pyrophosphorylase. Molecules and Cells, 29(4): 397–405

Kowalski G M, De Souza D P, Burch M L, Hamley S, Kloehn J, Selathurai A, Tull D, O'Callaghan S, McConville M J, Bruce C R (2015). Application of dynamic metabolomics to examine *in vivo* skeletal muscle glucose metabolism in the chronically high-fat fed mouse. Biochemical and Biophysical Research Communications, 462(1): 27–32

Krycer J R, Yugi K, Hirayama A, Fazakerley D J, Quek L E, Scalzo R, Ohno S, Hodson M P, Ikeda S, Shoji F, et al. (2017). Dynamic metabolomics reveals that insulin primes the adipocyte for glucose metabolism. Cell Reports, 21(12): 3536–3547

Kunz N, Camm E J, Somm E, Lodygensky G, Darbre S, Aubert M L, Hüppi P S, Sizonenko S V, Gruetter R (2011). Developmental and metabolic brain alterations in rats exposed to bisphenol A during gestation and lactation. International Journal of Developmental Neuroscience, 29(1): 37–43

Lai Y, Liu C W, Yang Y, Hsiao Y C, Ru H, Lu K (2021). High-coverage metabolomics uncovers microbiota-driven biochemical landscape of interorgan transport and gut-brain communication in mice. Nature Communications, 12(1): 6000

Lee H J, Jedrychowski M P, Vinayagam A, Wu N, Shyh-Chang N, Hu Y, Min-Wen C, Moore J K, Asara J M, Lyssiotis C A, Perrimon N, Gygi S P, Cantley L C, Kirschner M W (2017). Proteomic and metabolomic characterization of a mammalian cellular transition from quiescence to proliferation. Cell Reports, 20(3): 721–736

Li L, Hoefsloot H, Graaf A, Acar E, Smilde A (2021). Exploring dynamic metabolomics data with multiway data analysis: a simulation study. BMC Bioinformatics 23, 31 (2022)

Liang L, Rasmussen M H, Piening B, Shen X, Chen S, Rost H, Melbye M (2020). Metabolic dynamics and prediction of gestational age and time to delivery in pregnant women. Cell, 181(7): 1680–1692

Link H, Fuhrer T, Gerosa L, Zamboni N, Sauer U (2015). Real-time metabolome profiling of the metabolic switch between starvation and growth. Nature Methods, 12(11): 1091–1097

Link H, Kochanowski K, Sauer U (2013). Systematic identification of allosteric protein-metabolite interactions that control enzyme activity *in vivo*. Nature Biotechnology, 31(4): 357–361

Liu M, Jia S, Dong T, Zhao F, Xu T, Yang Q, Gong J, Fang M (2020). Metabolomic and transcriptomic analysis of MCF-7 cells exposed to 23 chemicals at human-relevant levels: estimation of individual chemical contribution to effects. Environmental Health Perspectives, 128(12): 127008

Liu M, Jiang J, Zheng J, Huan T, Gao B, Fei X, Wang Y, Fang M (2021). RTP: one effective platform to probe reactive compound transformation products and its applications for a reactive plasticizer BADGE. Environmental Science & Technology, 55(23): 16034–16043

Lu H, Chen H, Tang X, Yang Q, Zhang H, Chen Y Q, Chen W (2020). Time-resolved multi-omics analysis reveals the role of nutrient stress-induced resource reallocation for TAG accumulation in oleaginous fungus *Mortierella alpina*. Biotechnology for Biofuels,

13(1): 116

Luan H, Zhao H, Li J, Zhou Y, Fang J, Liu H, Li Y, Xia W, Xu S, Cai Z (2021). Machine learning for investigation on endocrine-disrupting chemicals with gestational age and delivery time in a longitudinal cohort. Research (Wash D C), 2021: 1

Lv Y, Wang X, Li X, Xu G, Bai Y, Wu J, Piao Y, Shi Y, Xiang R, Wang L (2020). Nucleotide de novo synthesis increases breast cancer stemness and metastasis via cGMP-PKG-MAPK signaling pathway. PLoS Biology, 18(11): e3000872

Mazat J P, Ransac S (2019). The fate of glutamine in human metabolism: the interplay with glucose in Proliferating cells. Metabolites, 9(5): 81

Meli R, Monnolo A, Annunziata C, Pirozzi C, Ferrante M C (2020). Oxidative stress and BPA toxicity: an antioxidant approach for male and female reproductive dysfunction. Antioxidants (Basel), 9(5): 405

Metallo C M, Vander Heiden M G (2013). Understanding metabolic regulation and its influence on cell physiology. Molecular Cell, 49(3): 388–398

Moffatt B A, Ashihara H (2002). Purine and pyrimidine nucleotide synthesis and metabolism. Arabidopsis Book, 1: 0018

Moreira J D, Hamraz M, Abolhassani M, Bigan E, Pérès S, Paulevé L, Nogueira M L, Steyaert J M, Schwartz L (2016). The redox status of cancer cells supports mechanisms behind the warburg effect. Metabolites, 6(4): 33

Moreno-Sánchez R, Saavedra E, Rodríguez-Enríquez S, Olín-Sandoval V (2008). Metabolic control analysis: a tool for designing strategies to manipulate metabolic pathways. Journal of Biomedicine & Biotechnology, 2008: 597913

Nyamundanda G, Gormley I C, Brennan L (2014). A dynamic probabilistic principal components model for the analysis of longitudinal metabolomics data. Applied Statistics, 63(5): 763–782

Ortiz-Villanueva E, Navarro-Martín L, Jaumot J, Benavente F, Sanz-Nebot V, Piña B, Tauler R (2017). Metabolic disruption of Zebrafish (*Danio rerio*) embryos by bisphenol A: an integrated metabolomic and transcriptomic approach. Environmental Pollution, 231(Pt 1): 22–36

Owen J B, Butterfield D A (2010). Measurement of oxidized/reduced glutathione ratio. Methods in Molecular Biology (Clifton, N.J.), 648: 269–277

Peng B, Zhao H, Keerthisinghe T P, Yu Y, Chen D, Huang Y, Fang M (2022). Gut microbial metabolite p-cresol alters biotransformation of bisphenol A: Enzyme competition or gene induction? Journal of Hazardous Materials, 426: 128093

Petroff O A C (2007). Metabolic Biopsy of the Brain. In: S. G. Waxman, ed. Molecular Neurology, 77–100. San Diego: Academic Press

Potratz S, Tarnow P, Jungnickel H, Baumann S, von Bergen M, Tralau T, Luch A (2017). Combination of metabolomics with cellular assays reveals new biomarkers and mechanistic insights on xenoestrogenic exposures in MCF-7 cells. Chemical Research in Toxicology, 30(4): 883–892

Quéméneur L, Gerland L M, Flacher M, Ffrench M, Revillard J P, Genestier L (2003). Differential control of cell cycle, proliferation, and survival of primary T lymphocytes by purine and pyrimidine nucleotides. Journal of Immunology (Baltimore, Md.: 1950), 170(10): 4986–4995

Rinschen M M, Ivanisevic J, Giera M, Siuzdak G (2019). Identification of bioactive metabolites using activity metabolomics. Nature Reviews. Molecular Cell Biology, 20(6): 353–367

Schymanski E L, Jeon J, Gulde R, Fenner K, Ruff M, Singer H P, Hollender J (2014). Identifying small molecules via high resolution mass spectrometry: communicating confidence. Environmental Science & Technology, 48(4): 2097–2098

Slominski A, Zmijewski M, Pawelek J (2012). L-tyrosine and L-dihydroxyphenylalanine as hormone-like regulators of melanocyte functions. Pigment Cell & Melanoma Research, 25(1): 14–27

Smilde A K, Westerhuis J A, Hoefsloot H C, Bijlsma S, Rubingh C M, Vis D J, Jellema R H, Pijl H, Roelfsema F, van der Greef J (2010). Dynamic metabolomic data analysis: a tutorial review. Metabolomics, 6(1): 3–17

Smith C A, O'Maille G, Want E J, Qin C, Trauger S A, Brandon T R, Custodio D E, Abagyan R, Siuzdak G (2005). METLIN: a metabolite mass spectral database. Therapeutic Drug Monitoring, 27(6): 747–751

Smith C A, Want E J, O'Maille G, Abagyan R, Siuzdak G (2006). XCMS: processing mass spectrometry data for metabolite profiling using nonlinear peak alignment, matching, and identification. Analytical Chemistry, 78(3): 779–787

Spégel P, Sharoyko V V, Goehring I, Danielsson A P, Malmgren S, Nagorny C L, Andersson L E, Koeck T, Sharp G W, Straub S G, Wollheim C B, Mulder H (2013). Time-resolved metabolomics analysis of β-cells implicates the pentose phosphate pathway in the control of insulin release. Biochemical Journal, 450(3): 595–605

Sweeney K J, Swarbrick A, Sutherland R L, Musgrove E A (1998). Lack of relationship between CDK activity and G1 cyclin expression in breast cancer cells. Oncogene, 16(22): 2865–2878

Tugizimana F, Djami-Tchatchou A T, Fahrmann J F, Steenkamp P A, Piater L A, Dubery I A (2019). Time-resolved decoding of metabolic signatures of *in vitro* growth of the hemibiotrophic pathogen *Colletotrichum sublineolum*. Scientific Reports, 9(1): 3290

Vahdati Hassani F, Abnous K, Mehri S, Jafarian A, Birner-Gruenberger R, Yazdian Robati R, Hosseinzadeh H (2018). Proteomics and phosphoproteomics analysis of liver in male rats exposed to bisphenol A: Mechanism of hepatotoxicity and biomarker discovery. Food and Chemical Toxicology, 112: 26–38

West P R, Weir A M, Smith A M, Donley E L, Cezar G G (2010). Predicting human developmental toxicity of pharmaceuticals using human embryonic stem cells and metabolomics. Toxicology and Applied Pharmacology, 247(1): 18–27

Wu G, Fang Y Z, Yang S, Lupton J R, Turner N D (2004). Glutathione metabolism and its implications for health. J Nutr, 134(3): 489–492

Wu J, Jin Z, Zheng H, Yan L J (2016). Sources and implications of NADH/NAD^+ redox imbalance in diabetes and its complications. Diabetes, Metabolic Syndrome and Obesity, 9: 145–153

Wu J, Wang F, Xie G, Cai Z (2022). Mass spectrometric determination of N7-HPTE-dG and N7-HPTE-Gua in mammalian cells and mice exposed to methoxychlor, an emergent persistent organic pollutant. Journal of Hazardous Materials, 432: 128741

Xu T, Chen L, Lim Y T, Zhao H, Chen H, Chen M W, Huan T, Huang Y, Sobota R M, Fang M (2021a). System biology-guided chemical

proteomics to discover protein targets of monoethylhexyl phthalate in regulating cell cycle. Environmental Science & Technology, 55(3): 1842–1851

Xu T, Lim Y T, Chen L, Zhao H, Low J H, Xia Y, Sobota R M, Fang M (2020). A novel mechanism of monoethylhexyl phthalate in lipid accumulation via inhibiting fatty acid beta-oxidation on hepatic cells. Environmental Science & Technology, 54(24): 15925–15934

Xu T, Zhao H, Wang M, Chow A, Fang M (2021b). Metabolomics and in *Silico* docking-directed discovery of small-molecule enzyme targets. Analytical Chemistry, 93(6): 3072–3081

Xu X, Wang L, Zang Q, Li S, Li L, Wang Z, He J, Qiang B, Han W, Zhang R, Peng X, Abliz Z (2021). Rewiring of purine metabolism in response to acidosis stress in glioma stem cells. Cell Death & Disease, 12(3): 277

Yanes O, Clark J, Wong D M, Patti G J, Sánchez-Ruiz A, Benton H P, Trauger S A, Desponts C, Ding S, Siuzdak G (2010). Metabolic oxidation regulates embryonic stem cell differentiation. Nature Chemical Biology, 6(6): 411–417

Yin J, Ren W, Huang X, Deng J, Li T, Yin Y (2018). Potential mechanisms connecting purine metabolism and cancer therapy. Frontiers in Immunology, 9: 1697

Yuan C, Zhang Y, Liu Y, Zhang T, Wang Z (2016). Enhanced GSH synthesis by bisphenol A exposure promoted DNA methylation process in the testes of adult rare minnow *Gobiocypris rarus*. Aquatic Toxicology (Amsterdam, Netherlands), 178: 99–105

Yue S, Yu J, Kong Y, Chen H, Mao M, Ji C, Shao S, Zhu J, Gu J, Zhao M (2019). Metabolomic modulations of HepG2 cells exposed to bisphenol analogues. Environment International, 129: 59–67

Zamboni N, Fendt S M, Rühl M, Sauer U (2009). ^{13}C-based metabolic flux analysis. Nature Protocols, 4(6): 878–892

Zampieri M, Sekar K, Zamboni N, Sauer U (2017). Frontiers of high-throughput metabolomics. Current Opinion in Chemical Biology, 36: 15–23

Zeng T, Liang Y, Dai Q, Tian J, Chen J, Lei B, Yang Z, Cai Z (2022). Application of machine learning algorithms to screen potential biomarkers under cadmium exposure based on human urine metabolic profiles. Chinese Chemical Letters, doi:

Zhang W, Zhou L, Yin P, Wang J, Lu X, Wang X, Chen J, Lin X, Xu G (2015). A weighted relative difference accumulation algorithm for dynamic metabolomics data: long-term elevated bile acids are risk factors for hepatocellular carcinoma. Scientific Reports, 5(1): 8984

Zhao F, Li L, Chen Y, Huang Y, Keerthisinghe T P, Chow A, Dong T, Jia S, Xing S, Warth B, Huan T, Fang M (2021). Risk-based chemical ranking and generating a prioritized human exposome database. Environmental Health Perspectives, 129(4): 047014

Zhao H, Liu M, Lv Y, Fang M (2022). Dose-response metabolomics and pathway sensitivity to map molecular cartography of bisphenol A exposure. Environment International, 158: 106893

Zimmer B M, Barycki J J, Simpson M A (2021). Integration of sugar metabolism and proteoglycan synthesis by UDP-glucose dehydrogenase. Journal of Histochemistry and Cytochemistry, 69(1): 13–23